Active anti-roll bar control using electronic servo valve hydraulic damper on single unit heavy vehicle

Van Tan Vu * **Olivier Sename** * **Luc Dugard** * **Peter Gaspar** **

* *Univ. Grenoble Alpes, GIPSA-lab, F-38402 Grenoble Cedex, France CNRS, GIPSA-lab, F-38402 Grenoble Cedex, France. E-mail: {Van-Tan.Vu, olivier.sename, luc.dugard}@gipsa-lab.grenoble-inp.fr*
** *Systems and Control Laboratory, Institute for Computer Science and Control, Hungarian Academy of Sciences, Kende u. 13-17, H-1111 Budapest, Hungary. E-mail: gaspar@sztaki.mta.hu*

Abstract: Rollover is a very serious problem for heavy vehicle safety, which can result in large financial and environmental consequences. In order to improve roll stability, most of modern heavy vehicles are equipped with passive anti-roll bars to reduce roll motion during cornering or riding on uneven roads. This paper introduces the active anti-roll bars designed by finding an optimal control based on a linear quadratic regulator (LQR). Four electronic servo valve hydraulic dampers are modelled and applied on a yaw roll model of a single unit heavy vehicle. The control signal is the current entering the electronic servo valve and the output of this actuator is the damping force generated by the hydraulic damper. Simulation results are obtained and compared in three different situations: without anti-roll bars, with passive anti-roll bars and with active anti-roll bars. It is shown that the use of two active (front and rear) anti-roll bars drastically improves the behaviour of the single unit heavy vehicle.

Keywords: Active anti-roll bar control, electronic servo valve hydraulic damper, rollover, roll stability, LQR control.

1. INTRODUCTION

1.1 Background

The rollover of heavy vehicle is an important road safety problem world-wide. Although rollovers are relatively rare events, they are usually deadly accidents when they occur. The main cause of traffic accidents in which heavy vehicles are involved is the roll stability loss. The three major contributing factors to rollover accidents are side wind gusts, abrupt steering and braking manoeuvres by the driver. In all these cases, roll stability loss is caused when the tire-road contact force on one of the side wheels becomes zero. It is well known that heavy vehicles have relatively high centres of mass and narrow track widths and can loose roll stability at moderate levels of lateral acceleration. Roll stability refers to the ability of a vehicle to overcome overturning moments generated during cornering and lane changing to avoid obstacle.

Currently, most of the heavy vehicles are equipped with passive anti-roll bars in all axles in order to improve roll stability. The passive anti-roll bar is usually made of steel and acts like a spring connected to the right and left wheels with chassis body. The passive anti-roll bar force is a function of the difference between right and left suspension deflections. The force is applied by the bar on each side of the vehicle so that the left force has the same magnitude as and the opposite direction to the right one. The passive anti-roll bar has the advantages to reduce the body roll acceleration and roll angle during single wheel lifting and cornering maneuvers. By reducing body roll motion, the driving safety and roll stability will be highly improved. However, the passive anti-roll bar also has disadvantages. During cornering maneuver, anti-roll bar will transfer vertical forces of one side of suspension to the other one, creating therefore a moment against lateral force (see Zulkarnain et al. (2012)).

In order to overcome the disadvantages of passive anti-roll bar, three main schemes concerned with the possible active intervention into the vehicle dynamics have been proposed: active steering, active brake and active anti-roll bar.

One of the methods proposed in the literature employs active steering: an actuator sets a small auxiliary front wheel steering angle in addition to the steering angle commanded by the driver. The aim is to decrease the rollover risk due to the transient roll overshoot of the vehicle when changing lanes or avoiding obstacles. However the active steering control also modifies the desired path of the vehicle, affecting the yaw motion (see Gaspar et al. (2004); Gaspar et al. (2005a)).

In the second method, the electronic brake mechanism with a small brake force is applied to each of the wheels and the slip response is monitored. In this way, it is possible to establish whether a given wheel is lightly loaded and the lift-off is imminent. When a dangerous situation is detected, unilateral brake forces are activated to reduce the lateral tire forces acting on the outside wheel. The brake system reduces directly the lateral tire force, which is responsible for the rollover. The active brake system is activated when the wheel reaches nearly the limit of lift-off (see Gaspar et al. (2004)).

In the third method, the active anti-roll bar is proposed by using a pair of hydraulic actuators (see Sampson and Cebon (2003); Gaspar et al. (2004), Zulkarnain et al. (2014)). Lateral acceleration makes vehicles with conventional passive suspension tilt out of corners. The center of the sprung mass shifts outboard of the vehicle centerline, which creates a destabilizing moment that reduces roll stability. The lateral load response is reduced by active anti-roll bars, which generate a stabilizing moment to counterbalance the overturning moment in such a way that the control torque leans the vehicle into the corners (see Zulkarnain et al. (2012)).

1.2 Related works

Most studies on active anti-roll bar systems use the damping force (or torque) as the input control signal. Miege and Cebon (2002) modelled and used a servo valve hydraulic actuator on the roll model and the input control signal is the spool valve of servo valve. In Varga et al. (2013) an electro-hydraulic actuator is applied on the roll model of a light commercial vehicle where the input control signal is the current, and the output is the torque of actuator.
Some of the control methods applied for active anti-roll bar control are briefly presented below:
In Sampson and Cebon (1998), Sampson and Cebon (2002), a basic state feedback controller was designed by finding an optimal controller based on a linear quadratic regulator (LQR) on the single unit heavy vehicle and an articulated heavy vehicle.
In Gaspar et al. (2005a), Gaspar et al. (2004) and Gaspar et al. (2005b), a fault detection and identification (FDI) filter, which identifies different actuator failures and a linear parameter varying (LPV) are used on the single unit heavy vehicle. The active anti-roll bar control is combined with an active brake control.
In Yu et al. (2008), the proposed rollover threat warning system uses the real-time dynamic model-based time-to-rollover (TTR) metric as a basis for online rollover detection.
In Boada et al. (2007), a reinforcement learning algorithm using neural networks to improve the roll stability in a single unit heavy vehicle is proposed.
In Zulkarnain et al. (2014), a LQG CNF fusion control strategy for an active anti-roll bar system is used to improve vehicle ride and handling.
The semi-active anti-roll system is also used, with a high and low roll stiffness (see Stone and Cebon (2010)).

1.3 Paper contribution

The paper contribution is twofold:
- First an integrated model, including an electronic servo valve hydraulic damper model and a heavy vehicle yaw roll model, is proposed to control the spool valve displacement which distributes high pressure oil into two chambers of the hydraulic cylinder. The input current of the electronic servo valve is controlled to generate the damping force in various maneuver situations.
The use of the electronic servo valve hydraulic damper on a yaw roll model of a single unit heavy vehicle is an evolution compared to previous studies.
- Then an optimal LQR is developed where the optimal criterion is formulated from the vehicle dynamics specifications (in terms of comfort or road handling). The proposed generic definition of the control law allows to cope with most of the industrial performance requirements.
The paper is organised as follows: Section 2 gives the integrated model of heavy vehicle. Section 3 presents the design of the passive anti-roll bar. Section 4 gives the active anti-roll bar designed by finding an optimal control based on a LQR. Section 5 illustrates the approach by giving an example where the passive anti-roll bar and the LQR active anti-roll bar controls are compared with the case without anti-roll bar. Finally, some conclusions are drawn in section 6.

2. INTEGRATED MODEL OF HEAVY VEHICLE

The integrated model includes an electronic servo-valve hydraulic damper model and a heavy vehicle yaw roll model.

2.1 Electronic servo valve hydraulic damper model

Figure 1 illustrates the diagram of the electronic servo valve hydraulic damper. It consists of an electronic servo valve (or proportional valve) and a hydraulic cylinder.

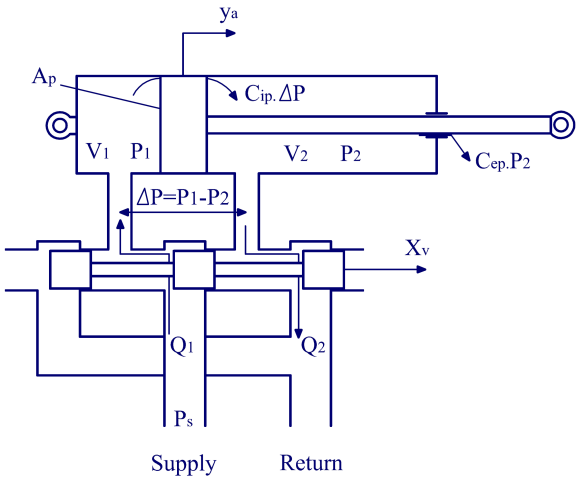

Fig. 1. Diagram of the electronic servo valve hydraulic damper.

The spool valve of electronic servo valve is controlled by current which generates displacement X_v. The high pressure oil P_s is always stored outside the electronic servo-valve and the moving spool-valve will distribute high pressure oil into two chambers of the hydraulic cylinder. The difference of pressure ΔP in the two chambers produces the output damping force F_{act} given by:

$$F_{act} = A_P \Delta P \tag{1}$$

where A_P is the area of the piston.
The servo-valve orifices are assumed to be matched and symmetrical, so that the load flow Q_L (see Miege and Cebon (2002)) is computed as follows:

$$Q_L = \frac{Q_1 + Q_2}{2} = K_x X_v - K_p \Delta P \tag{2}$$

where K_x and K_P are the valve flow gain and pressure coefficient, respectively.
The equations for each chamber can be written as:

$$\begin{cases} Q_1 - C_{ip}(P_1 - P_2) - C_{ep} P_1 = \dfrac{dV_1}{dt} + \dfrac{V_1}{\beta_e}\dfrac{dP_1}{dt} \\ C_{ip}(P_1 - P_2) - C_{ep} P_2 - Q_2 = \dfrac{dV_2}{dt} + \dfrac{V_2}{\beta_e}\dfrac{dP_2}{dt} \end{cases}$$

where β_e is the effective bulk modulus of the oil, C_{ep} and C_{ip} are the external and internal leakage coefficients of the damper. The volume in each chamber varies with the piston displacement as:

$$\begin{cases} V_1 = V_{01} + A_p y_a \\ V_2 = V_{02} - A_p y_a \end{cases}$$

where V_{01} and V_{02} are the initial volumes in each chamber, y_a is the piston (damper) displacement. With the assumption that $V_{01} = V_{02} = V_0$, the total volume of trapped oil is given by:

$$V_t = V_1 + V_2 = V_{01} + V_{02} = 2V_0$$

Therefore, the equations in each chamber become:

$$\begin{cases} Q_1 - C_{ip}(P_1 - P_2) - C_{ep} P_1 = A_p \dfrac{dy_a}{dt} + \dfrac{V_0 + A_p y_a}{\beta_e}\dfrac{dP_1}{dt} \\ C_{ip}(P_1 - P_2) - C_{ep} P_2 - Q_2 = -A_p \dfrac{dy_a}{dt} + \dfrac{V_0 - A_p y_a}{\beta_e}\dfrac{dP_2}{dt} \end{cases}$$

Subtracting the second equation from the first one gives:

$$Q_L = C_{tp}\Delta P + A_p \frac{dy_a}{dt} + \frac{V_0}{2\beta_e}\frac{d\Delta P}{dt} \tag{3}$$

where C_{tp} is the total leakage coefficient of the damper.
From equations (2) and (3), the dynamic equation of the servo valve hydraulic damper is as follows:

$$\frac{V_t}{4\beta_e}\frac{d\Delta P}{dt} + (K_P + C_{tp})\Delta P - K_x X_v + A_P \frac{dy_a}{dt} = 0 \tag{4}$$

The displacement of the spool valve X_v is controlled by current u. The effects of hysteresis and flow forces on the servo-valve are neglected, then the dynamic behavior of the electronic servo-valve can be approximated by a first-order model (see Rafa et al. (2009)), as follows:

$$\frac{dX_v}{dt} + \frac{1}{\tau}X_v - \frac{K_v}{\tau}u = 0 \tag{5}$$

where τ is the time constant and K_v the gain of the servo-valve.
The equations (1), (4), (5) are the dynamic equations of the electronic servo valve hydraulic damper, where the input signal is the current u and the output is the damping force F_{act}.
The parameters of the electronic servo valve hydraulic damper are shown in table 1.

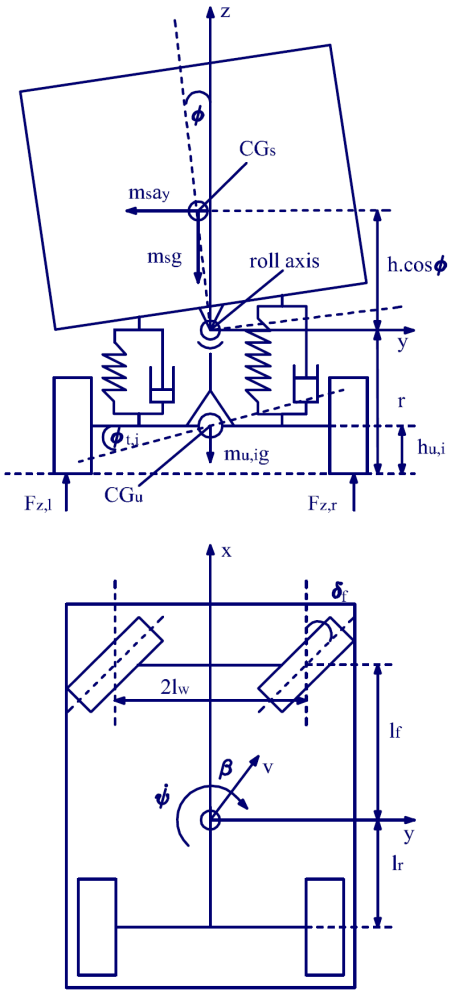

Fig. 2. Yaw-Roll model of single unit heavy vehicle.

2.2 *Yaw-roll model of single unit heavy vehicle*

Fig 2 illustrates the combined yaw-roll dynamics of the vehicle modelled by a three-body system, in which m_s is the sprung mass, m_{uf} is the unsprung mass at the front including the front wheels and axle, and m_{ur} is the unsprung mass at the rear with the rear wheels and axle. The parameters and variables of the yaw roll model are shown in the table 2.

Table 1. Parameters of the electronic servo valve hydraulic damper (see Miege and Cebon (2002), Rafa et al. (2009)).

Symbols	Description	Value	Unit
A_P	Area of the piston	0.0123	m^2
K_x	Valve flow gain coefficient	2.5	m^2/s
K_P	Total flow pressure coefficient	$4.2x10^{-11}$	$m^5/(Ns)$
C_{tp}	Total leakage coefficient of the damper	0	-
V_t	Total volume of trapped oil	0.0014	m^3
β_e	Effective bulk modulus of the oil	$6.89x10^6$	N/m^2
τ	Time constant of the servo valve	0.01	s
K_v	Servo valve gain	0.955	$in./A$

Table 2. Parameters of the yaw-roll model (see Gaspar et al. (2005a))

Symbols	Description	Value	Unit
m_s	Sprung mass	12487	kg
$m_{u,f}$	Unsprung mass on the front axle	706	kg
$m_{u,r}$	Unsprung mass on the rear axle	1000	kg
m	The total vehicle mass	14193	kg
v	Forward velocity	-	$\frac{Km}{h}$
v_{wi}	Components of the forward velocity	-	$\frac{Km}{h}$
h	Height of CG of sprung mass from roll axis	1.15	m
$h_{u,i}$	Height of CG of unsprung mass from ground	0.53	m
r	Height of roll axis from ground	0.83	m
a_y	Lateral acceleration	-	$\frac{m}{s^2}$
β	Side-slip angle at center of mass	-	rad
ψ	Heading angle	-	rad
$\dot{\psi}$	Yaw rate	-	$\frac{rad}{s}$
α	Side slip angle	-	rad
ϕ	Sprung mass roll angle	-	rad
$\phi_{t,i}$	Unsprung mass roll angle	-	rad
δ_f	Steering angle	-	rad
u_i	Control current	-	A
C_f	Tire cornering stiffness on the front axle	582	$\frac{kN}{rad}$
C_r	Tire cornering stiffness on the rear axle	783	$\frac{kN}{rad}$
k_f	Suspension roll stiffness on the front axle	380	$\frac{kNm}{rad}$
k_r	Suspension roll stiffness on the rear axle	684	$\frac{kNm}{rad}$
b_f	Suspension roll damping on the front axle	100	$\frac{kN}{rad}$
b_r	Suspension roll damping on the rear axle	100	$\frac{kN}{rad}$
k_{tf}	Tire roll stiffness on the front axle	2060	$\frac{kNm}{rad}$
k_{tr}	Tire roll stiffness on the rear axle	3337	$\frac{kNm}{rad}$
I_{xx}	Roll moment of inertia of sprung mass	24201	kgm^2
I_{xz}	Yaw-roll product of inertial of sprung mass	4200	kgm^2
I_{zz}	Yaw moment of inertia of sprung mass	34917	kgm^2
l_f	Length of the front axle from the CG	1.95	m
l_r	Length of the rear axle from the CG	1.54	m
l_w	Half of the vehicle width	0.93	m
μ	Road adhesion coefficient	1	-
D_f	Outer diameter of front anti-roll bar	32	mm
D_r	Outer diameter of rear anti-roll bar	34	mm
E	Young's modulus of material	206000	MPa

In the vehicle modelling, the motion differential equations of the yaw-roll dynamics of the single unit vehicle, i.e. the lateral dynamics, the yaw moment, the roll moment of the sprung mass, the roll moment of the front and the rear unsprung

masses, are formalized in the equations (10).
When the vertical displacements of the left and the right wheels are different, the passive anti-roll bar with a rotational stiffness k_{AO} creates an anti-roll moment, resulting in the anti-roll force F_{AU}, see Figure 3, acting on the unsprung mass as:

$$F_{AUl} = -F_{AUr} = k_{AO}(\frac{\Delta Z_{Ar} - \Delta Z_{Al}}{c^2}) \tag{6}$$

and the anti-roll force F_{AS} acting on the sprung mass is:

$$F_{ASl} = -F_{ASr} = F_{AUl}\frac{t_A}{t_B} = k_{AO}(\Delta Z_{Ar} - \Delta Z_{Al})\frac{t_A}{t_B c^2} \tag{7}$$

where $\Delta Z_{Ar,l}$ are the displacements of the connection point between the anti-roll bars and the wheels, t_A is half the distance of the two suspensions, t_B is half the distance of the chassis, c is the length of the anti-roll bars's arm, k_{AU} and k_{AS} are the modified rotational stiffness corresponding to the unsprung and sprung mass, respectively:

$$k_{AU} = k_{AO}\frac{1}{c^2} \quad and \quad k_{AS} = k_{AO}\frac{t_A}{t_B c^2} \tag{8}$$

The moment of passive anti-roll bar impacts the unsprung mass and sprung mass as follows:

$$M_{AR} = 4k_{AO}\frac{t_A t_B}{c^2}\phi - 4k_{AO}\frac{t_A^2}{c^2}\phi_u \tag{9}$$

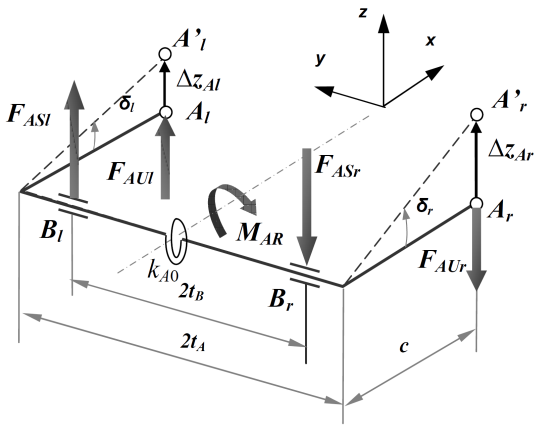

Fig. 3. Diagram of the passive anti-roll bars on the vehicles.

The motion differential equations of the yaw-roll model of the heavy vehicle are formalized as follows:

$$\begin{cases} mv(\dot\beta + \dot\psi) - m_s h\ddot\phi = F_{yf} + F_{yr} \\ -I_{xz}\ddot\phi + I_{zz}\ddot\psi = F_{yf}l_f - F_{yr}l_r \\ (I_{xx} + m_s h^2)\ddot\phi - I_{xz}\ddot\psi = m_s g h\phi + m_s v h(\dot\beta + \dot\psi) \\ \quad -k_f(\phi - \phi_{tf}) - b_f(\dot\phi - \dot\phi_{tf}) + M_{ARf} + U_f \\ \quad -k_r(\phi - \phi_{tr}) - b_r(\dot\phi - \dot\phi_{tr}) + M_{ARr} + U_r \\ -rF_{yf} = m_{uf}v(r - h_{uf})(\dot\beta + \dot\psi) + m_{uf}gh_{uf}.\phi_{tf} - k_{tf}\phi_{tf} \\ \quad +k_f(\phi - \phi_{tf}) + b_f(\dot\phi - \dot\phi_{tf}) + M_{ARf} + U_f \\ -rF_{yr} = m_{ur}v(r - h_{ur})(\dot\beta + \dot\psi) - m_{ur}gh_{ur}\phi_{tr} - k_{tr}\phi_{tr} \\ \quad +k_r(\phi - \phi_{tr}) + b_r(\dot\phi - \dot\phi_{tr}) + M_{ARr} + U_r \end{cases} \tag{10}$$

The lateral tire forces $F_{y;i}$ in the direction of velocity at the wheel ground contact points are considered, by approximation, proportional to the tire side slip angle α.

$$\begin{cases} F_{yf} = \mu C_f \alpha_f \\ F_{yr} = \mu C_r \alpha_r \end{cases}$$

The classic equations for the tire side slip angles are:

$$\begin{cases} \alpha_f = -\beta + \delta_f - \dfrac{l_f\dot\psi}{v} \\ \alpha_r = -\beta + \dfrac{l_r\dot\psi}{v} \end{cases}$$

In the integrated model of heavy vehicle, four electronic servo valve hydraulic dampers are used (two for the front axle and two for the rear one). In each axle, the forces of the two dampers have the same magnitude and the opposite direction. Therefore the torque generated by the active anti-roll bar system on the front axle is determined by:

$$U_f = 2l_{act}A_p\Delta_{Pf} \tag{11}$$

and for the torque generated by the active anti-roll bar system on the rear axle, one has:

$$U_r = 2l_{act}A_p\Delta_{Pr} \tag{12}$$

where l_{act} is half the distance of the two actuators. The equations of these electronic servo valve dampers are shown in equation (13).

$$\begin{cases} \dfrac{V_t}{4\beta_e}\dot\Delta_{Pf} + (K_P + C_{tp})\Delta_{Pf} - K_x X_{vf} \\ \quad +A_p l_{act}\dot\phi - A_p l_{act}\dot\phi_{uf} = 0 \\ \dot X_{vf} + \dfrac{1}{\tau}X_{vf} - \dfrac{K_v}{\tau}u_f = 0 \\ \dfrac{V_t}{4\beta_e}\dot\Delta_{Pr} + (K_P + C_{tp})\Delta_{Pr} - K_x X_{vf} \\ \quad +A_p l_{act}\dot\phi - A_p l_{act}\dot\phi_{ur} = 0 \\ \dot X_{vr} + \dfrac{1}{\tau}X_{vr} - \dfrac{K_v}{\tau}u_r = 0 \end{cases} \tag{13}$$

The motion differential equations (10) can be rewritten in the LTI state-space representation as:

$$\begin{cases} \dot X = A.X + B_1.W + B_2.U \\ Z = C.X + D_1.W + D_2.U \end{cases} \tag{14}$$

with the state vector:

$$X = \left[\, \beta \;\; \dot\psi \;\; \phi \;\; \dot\phi \;\; \phi_{tf} \;\; \phi_{tr} \;\; \Delta_{Pf} \;\; X_{vf} \;\; \Delta_{Pr} \;\; X_{vr} \,\right]^T$$

the exogenous disturbance:

$$W = \left[\, \delta_f \,\right]^T$$

the control input:

$$U = \left[\, u_f \;\; u_r \,\right]^T$$

the output vector:

$$Z = \left[\, \beta \;\; \dot\psi \;\; \phi \;\; \dot\phi \;\; \phi_{tf} \;\; \phi_{tr} \;\; \Delta_{Pf} \;\; X_{vf} \;\; \Delta_{Pr} \;\; X_{vr} \,\right]^T$$

3. DESIGN OF A PASSIVE ANTI-ROLL BAR

The design of an anti-roll bar actually means to obtain the required anti-roll stiffness that improves the vehicles stability and handling performance without exceeding the mechanic limitations of the bar material. See (Bharane et al. (2014); Caliskan (2003)) for general information about torsion bars and their manufacturing processing in Spring Design Manual. Anti-roll bars are dealt as a sub-group of torsion bars. Some useful formulae for calculating the torsional stiffness of anti-roll bars

and deflection at the end point of the bar under a given loading, are provided in the manual. However, the formulations can only be applied to the bars with standard shapes (simple, torsion bar shaped anti-roll bars). The applicable geometry is shown in Figure 4.

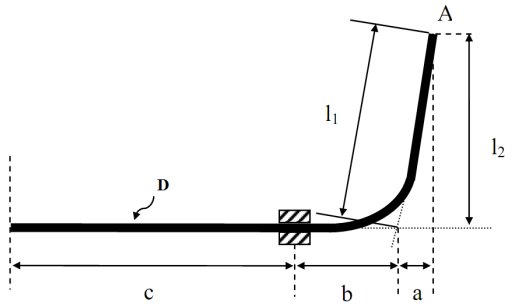

Fig. 4. Anti-roll bar geometry used in SAE Spring Design Manual.

The loading is applied at point A, inward to or outward from plane of the page. The roll stiffness of such a bar can be calculated as:

$$r = k_{AO} = \frac{PL^2}{2f_A} \tag{15}$$

where:
f_A - Deflection of point A:

$$f_A = \frac{P}{3EI}[l_1^3 - a^3 + \frac{L}{2}(a+b)^2 + 4l_2^2(b+c)] \tag{16}$$

L - Half track length of anti-roll bar:

$$L = a + b + c \tag{17}$$

I - Moment of inertia of anti-roll bar:

$$I = \pi\frac{D^4}{64} \tag{18}$$

with, D - Outer diameter, E - Young's modulus of material
The material of anti-roll bar is issued from SAE 5160 and the parameters of the passive anti-roll bar are given in table 2.
The torsional stiffness of the anti-roll bar on the front axle is:

$$r_f = k_{AOf} = 10730 \quad (\frac{Nm}{rad})$$

The torsional stiffness of the anti-roll bar on the rear axle is:

$$r_r = k_{AOr} = 15480 \quad (\frac{Nm}{rad})$$

4. ACTIVE ANTI-ROLL BAR CONTROL

The objective of the active anti-roll bar control system is to maximize the roll stability of the vehicle. The rollover is caused by the high lateral inertial force generated by lateral acceleration. If the position of the center of gravity is high or the forward velocity of the vehicle is larger than allowed at a given steering angle, the resulting lateral acceleration is also large and might initiate a rollover. An imminent rollover can be detected if the calculated lateral load transfer reaches 1 (or -1). The lateral load transfer can be given by:

$$\Delta F_z = \frac{k_u \phi_u}{l_w} \tag{19}$$

where k_u is the stiffness of tire, ϕ_u the roll angle of the unsprung mass and l_w the half of vehicle's width. The lateral load transfer can be normalized in such a way that the load transfer is divided by the total axle load F_z (see Gaspar et al. (2004)).

$$R = \frac{\Delta F_z}{F_z} \tag{20}$$

The normalized load transfer R value corresponds to the largest possible load transfer. If R takes on the value ± 1 then the inner wheel in the bend lift off.
The roll stability is achieved by limiting the lateral load transfer within the levels required for wheel lift-off. Specifically, the load transfer can be minimized to increase the inward lean of the vehicle. The center of mass shifts laterally from the nominal center line of the vehicle to provide a stabilizing effect. While attempting to minimize the load transfer, it is also necessary to constrain the roll angles between the sprung and unsprung mass $(\phi - \phi_u)$ so that they are within the limits of the travel of suspension $((7-8deg)$ see Gaspar et al. (2004)).
The performance characteristic which is of most interest when designing the active anti-roll bar, is the lateral load transfer R that the controller should minimize.
The linear time-invariant (LTI) model is described by equation (14). For controller design, it is assumed that all the states are available from measurements or can be estimated. First of all, let us consider the feedback control law:

$$u = -KX \tag{21}$$

where K is the state feedback gain matrix. The optimization procedure consists in determining the control input u, which minimizes some performance index J. This index includes the performance characteristic requirement as well as the controller input limitations, usually expressed by:

$$J = \int_0^\infty (\mathrm{x}^\mathrm{T}\mathrm{Q}\mathrm{x} + \mathrm{u}^\mathrm{T}\mathrm{R}\mathrm{u})\,\mathrm{d}t \tag{22}$$

where Q and R are positive definite weighting matrices. To obtain a solution for the optimal controller (21), the LTI system must be stabilizable, which is true for the model (14).
Linear optimal control theory provides the solution K that minimizes (22). The gain matrix K is computed from:

$$K = R^{-1}B^T P \tag{23}$$

where the matrix P is the solution of the Algebraic Riccati Equation (ARE):

$$AP + A^T P - PBR^{-1}B^T P + Q = 0 \tag{24}$$

The optimal closed-loop system is obtained with equations (14), (21) and (23) as follows:

$$\dot{X} = (A - B_2 K)X + B_1 W \tag{25}$$

As the objective of the controller is to maximize the roll stability of the vehicle, the performance index J is selected as follows:

$$J = \int_0^\infty (\rho_1\beta^2 + \rho_2\dot{\psi}^2 + \rho_3\phi^2 + \rho_4\dot{\phi}^2 + \rho_5{\phi_{\mathrm{uf}}}^2 + \rho_6{\phi_{\mathrm{ur}}}^2 + \rho_7{\Delta_{\mathrm{Pf}}}^2 + \rho_8{\mathrm{X}_{\mathrm{vf}}}^2 + \rho_9{\Delta_{\mathrm{Pr}}}^2 + \rho_{10}{\mathrm{X}_{\mathrm{vr}}}^2 + \mathrm{R}_1{\mathrm{u}_\mathrm{f}}^2 + \mathrm{R}_2{\mathrm{u}_\mathrm{r}}^2)\,\mathrm{d}t$$

To assess the quality of the active anti-roll bar control system, two controllers have been designed and compared:
- First controller: The roll stability is the most important objective. The coefficients of the performance index are chosen as:

$$\rho_1 = 0 \quad \rho_2 = 0 \quad \rho_3 = 100 \quad \rho_4 = 100 \quad \rho_5 = 100 \quad \rho_6 = 100$$
$$\rho_7 = 0 \quad \rho_8 = 0 \quad \rho_9 = 0 \quad \rho_{10} = 0 \quad R_1 = 10^{-2} \quad R_2 = 10^{-2}$$

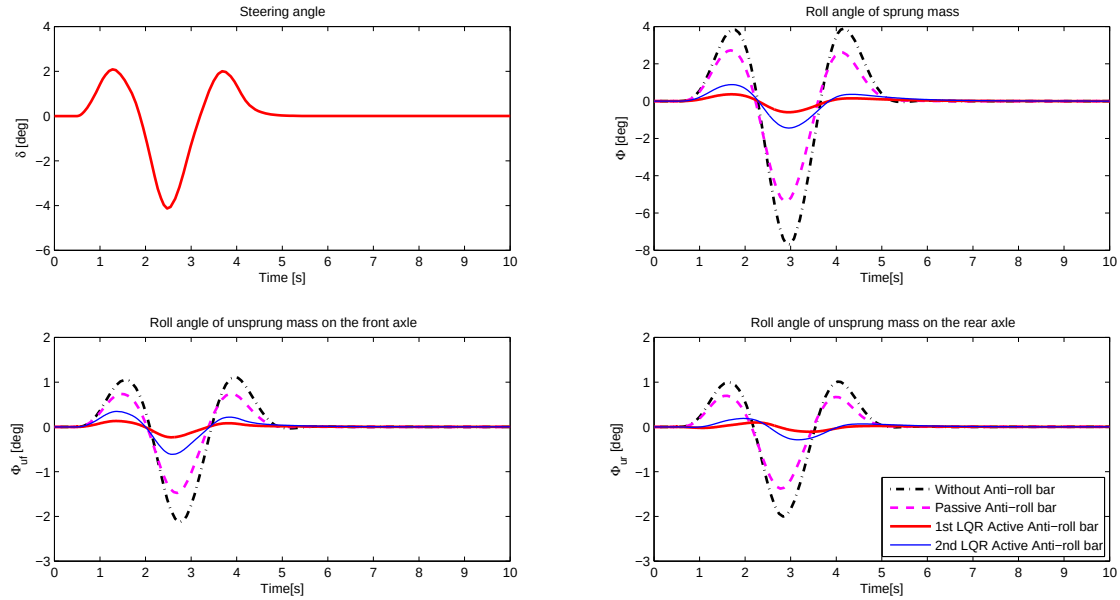

Fig. 5. Time responses of roll angle of sprung mass and unsprung mass of single unit heavy vehicle.

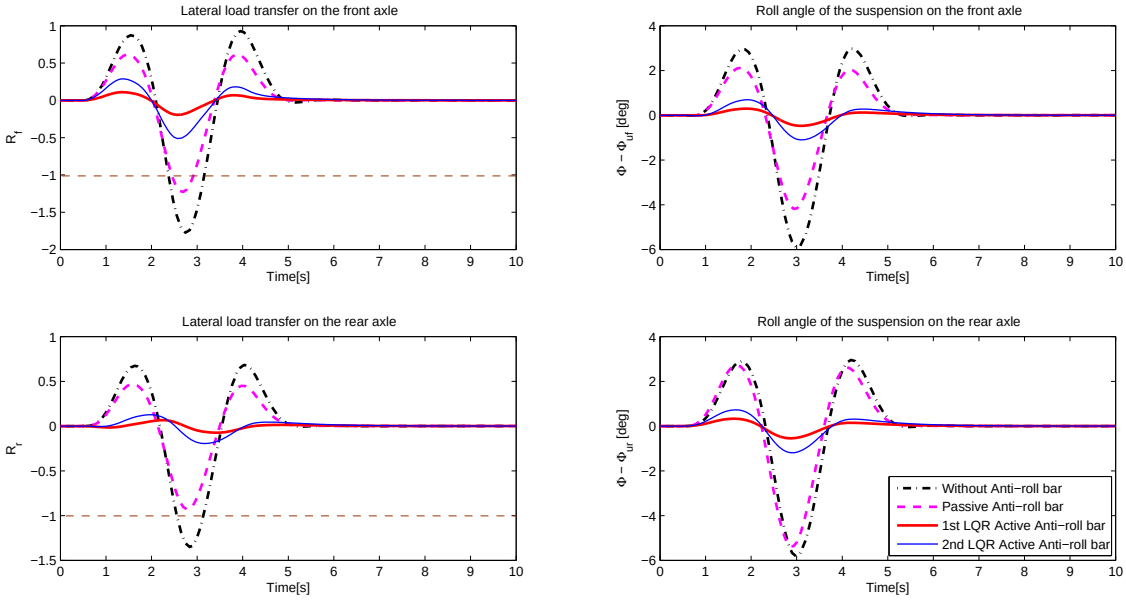

Fig. 6. Time responses of lateral load transfer and roll angle of suspension on the axles of single unit heavy vehicle.

- Second controller: The controller input limitations are more taken into account, while keeping the roll stability objective. The coefficients are then chosen as:

$$\rho_1 = 0 \quad \rho_2 = 0 \quad \rho_3 = 5 \quad \rho_4 = 5 \quad \rho_5 = 5 \quad \rho_6 = 5$$
$$\rho_7 = 0 \quad \rho_8 = 0 \quad \rho_9 = 0 \quad \rho_{10} = 0 \quad R_1 = 10^{-1} \quad R_2 = 10^{-1}$$

5. SIMULATION EXAMPLES

In this section, some results are shown for active anti-roll bar, designed in the previous section by finding an optimal control based on a linear quadratic regulator (LQR). Two pairs of electronic servo valve hydraulic dampers are used with the currents of electronic servo valves as input signals. The disturbance is the steering angle δ which is determined from Gaspar et al. (2004). The vehicle maneuver is a double lane change which is often used to avoid an obstacle in an emergency. The maneuver has a $2m$ path deviation over $100m$. The size of the path deviation is chosen to test a real obstacle avoidance in an emergency. The forward velocity is $70Km/h$. The parameters values of the electronic servo valve hydraulic damper and the yaw-roll model of single unit heavy vehicle are found in tables 1 and 2.
Figure 5 and figure 6 show the time responses for the first LQR active anti-roll bar (thick line), the second LQR active anti-roll bar (thin like), the passive anti-roll bar (dash line) and the without anti-roll bar (dash-dot line). The figure 5 shows the

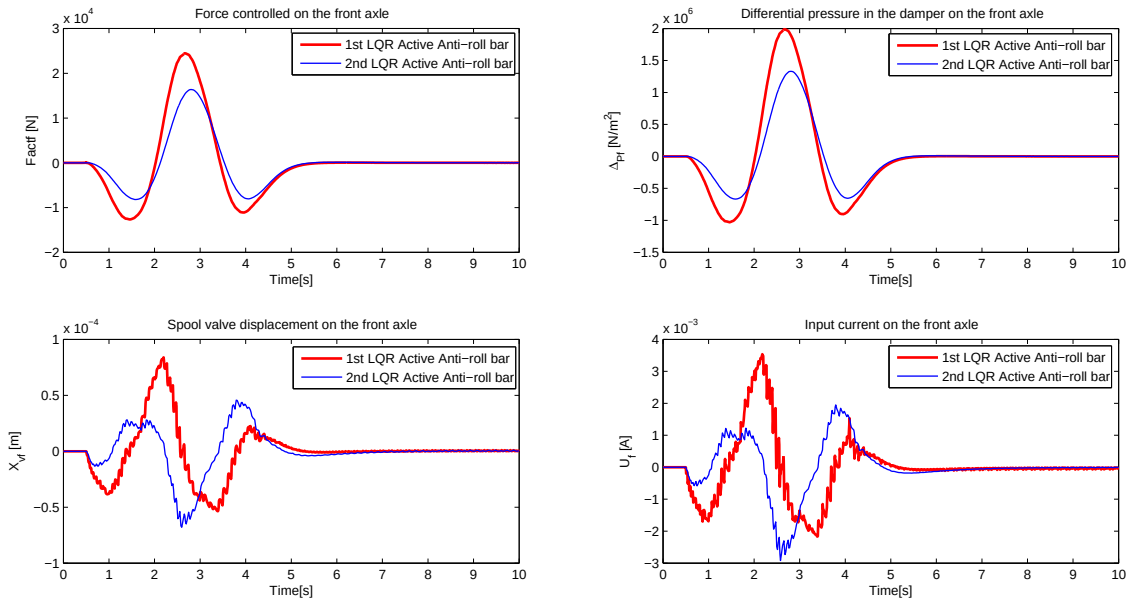

Fig. 7. The characteristics of the electronic servo valve hydraulic dampers on the **front** axle.

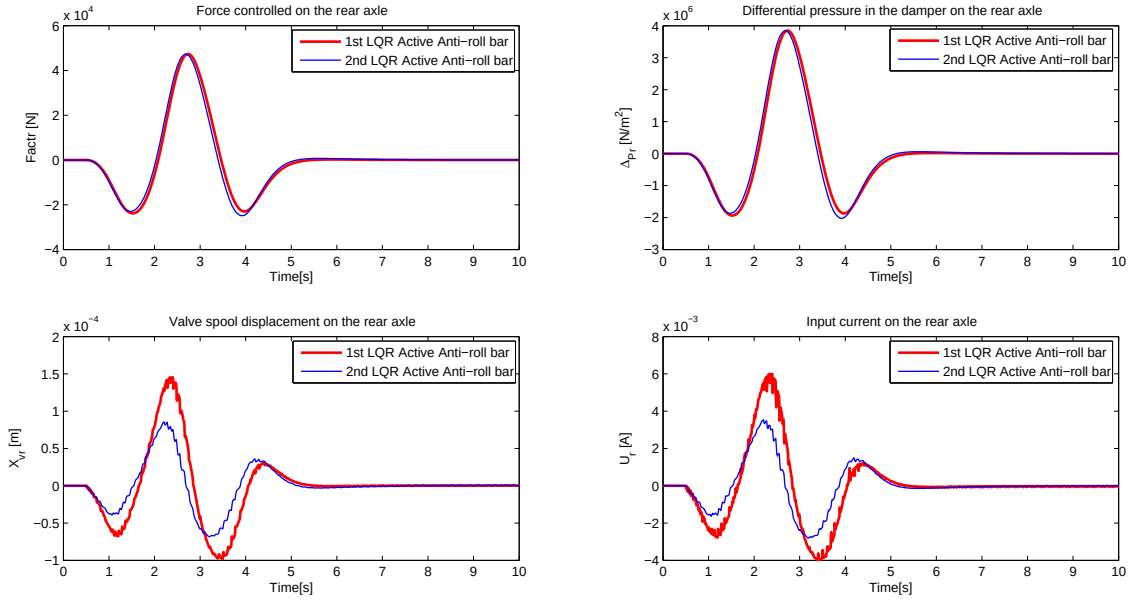

Fig. 8. The characteristics of the electronic servo valve hydraulic dampers on the **rear** axle.

steering angle δ, the roll angle of sprung mass ϕ, the roll angle of the unsprung mass at the front axle ϕ_{uf} and the roll angle of the unsprung mass at the rear axle ϕ_{ur}. The figure 6 shows the lateral load transfer and roll angle of suspension on the front and on the rear axle, respectively. We can see that the value of the lateral load transfers at 2.8 seconds exceeds -1 without anti-roll bar so that the inner wheels lift off. With the passive anti-roll bar, the lateral load transfer on the front axle exceeds -1, but on the rear axle this value is within the limit. For the LQR active anti-roll bar, the roll stability is achieved because the limits of the lateral load transfers always stay within ± 1. The maximum of the absolute values of the roll angle of the suspensions is always less than $(7-8deg)$, so that the roll angles of the suspensions are within the limits of the travel of suspension. From these figures, we can claim that the two active anti-roll bar controllers significantly enhance the roll stability of the heavy vehicle compared to both two cases without anti-roll bar and with the passive anti-roll bar. As explained with the choice of the parameters in the performance index J, the first active controller performs better than the second one, in term of roll stability.

The characteristics of the electronic servo valve hydraulic dampers on the front and rear axles, shown on figures 7 and 8, include: the damping force F_{act}, the differential pressure in the damper Δ_P, the valve spool displacement X_v and the input current u. From these figures, we can see that the second

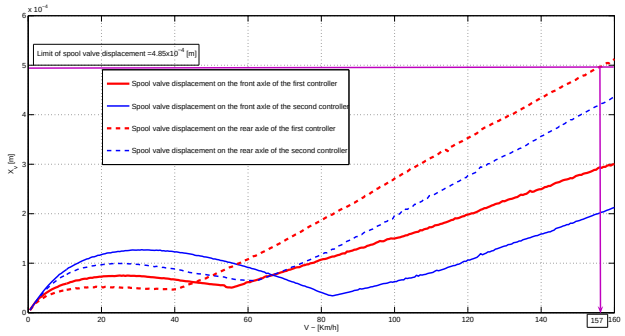

Fig. 9. The influence of forward velocity to the maximum of the absolute value of the spool valve displacement.

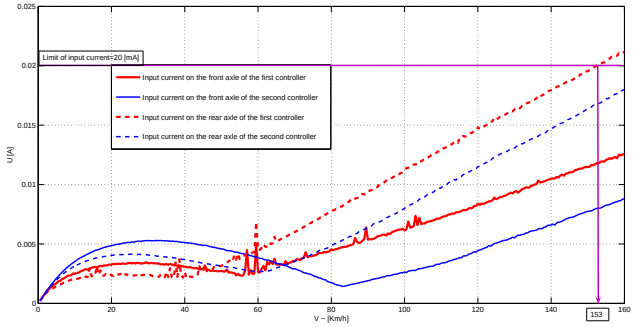

Fig. 10. The influence of forward velocity to the maximum of the absolute value of the input current.

controller has focused on reducing the input control signals w.r.t the first one; the difference is reflected in the characteristics of both axles.

Figure 9 shows that the maximal admissible limit for the forward velocity of the heavy vehicle is 157 Km/h in order to ensure that the spool valve displacement is kept within its limit ($4.85x10^{-4}m$).

As well, Figure 10 shows that the maximal admissible limit for the forward velocity of the heavy vehicle is 153 Km/h in order to ensure that the input current is kept within its limit ($20mA$).

6. CONCLUSION

The use of electronic servo valve hydraulic damper, where the input control signal is the current, is completely applicable for active anti-roll bar control system on the heavy vehicle as shown in the simulation section.

The active anti-roll bar control is based on the LQR control, and the lateral load transfer is taken into consideration. The obtained results have shown the effectiveness of the LQR active anti-roll bar control to improve the roll stability to prevent the rollover phenomenon of heavy vehicle, compared with the passive anti-roll bar and without anti-roll bar. In the future, robust control methods will be used and applied for active anti-roll bar control using the integrated model of single unit heavy vehicle.

REFERENCES

Bharane, P., Tanpure, K., Patil, A., and Kerkal, G. (2014). Design, analysis and optimization of anti-roll bar. *Journal of Engineering Research and Applications*, 4(9), 137–140.

Boada, M., Boada, B., Quesada, A., Gaucha, A., and Daz, V. (2007). Active roll control using reinforcement learning for a single unit heavy vehicle. In *12th IFToMM World Congress*. Besancon, France.

Caliskan, K. (2003). *Automated design analysis of anti-roll bars*. Ph.D. thesis, The Middle East Technical University.

Gaspar, P., Bokor, J., and Szaszi, I. (2004). The design of a combined control structure to prevent the rollver of heavy vehicles. *European Journal of Control*, 10(2), 148–162.

Gaspar, P., Bokor, J., and Szaszi, I. (2005a). Reconfigurable control structure to prevent the rollover of heavy vehicles. *Control Engineering Practice*, 13(6), 699–711.

Gaspar, P., Szabo, Z., and Bokor, J. (2005b). Prediction based combined control to prevent the rollover of heavy vehicles. In *Proceedings of the 13th Mediterranean Conference on Control and Automation*. Limassol, Cyprus.

Miege, A. and Cebon, D. (2002). Design and implementation of an active roll control system for heavy vehicles. In 6^{th} *International Symposium on Advanced Vehicle Control, AVEC 2002*. Hiroshima, Japan.

Rafa, A.H.A.B., Yahya, A.F., and Rawand, E.J.T. (2009). A study on the effects of servovalve lap on the performance of a closed - loop electrohydraulic position control system. *Al-Rafidain Engineering*, 17(5).

Sampson, D. and Cebon, D. (1998). An investigation of roll control system design for articulated heavy vehicles. In *4th International symposium on Advanced Vehicle Control, AVEC1998*. Nagoya, Japan.

Sampson, D. and Cebon, D. (2002). Achievable roll stability of heavy road vehicles. In *Proceedings of the Institution of Mechanical Engineers, Part D: Journal of Automobile Engineering*, volume 217. United Kingdom.

Sampson, D. and Cebon, D. (2003). Active roll control of single unit heavy road vehicles. *Vehicle System Dynamics: International Journal of Vehicle Mechanics and Mobility*, 40(4), 229–270.

Stone, E. and Cebon, D. (2010). Control of semi-active anti-roll systems on heavy vehicles. *Vehicle System Dynamics: International Journal of Vehicle Mechanics and Mobility*, 48(10), 1215–1243.

Varga, B., Nemeth, B., and Gaspar, P. (2013). Control Design of Anti-Roll Bar Actuator Based on Constrained LQ Method. In 14^{th} *IEEE International Symposium on Computational Intelligence and Informatics Conference*. Budapest, Hungary.

Yu, H., Guvenc, L., and Ozguner, U. (2008). Heavy duty vehicle rollover detection and active roll control. *Vehicle System Dynamics*, 46(6), 451–470.

Zulkarnain, N., Zamzuri, H., Sam, Y., Mazlan, S., and Zainal, S. (2014). Improving vehicle ride and handling using LQG CNF fusion control strategy for an active anti-roll bar system. *Hindawi Publishing Corporation*, 2014(1). doi:10.1155/2014/698195.

Zulkarnain, N., Imaduddin, F., Zamzuri, H., and Mazlan, S.A. (2012). Application of an active anti-roll bar system for enhancing vehicle ride and handling. In *2012 IEEE Colloquium on Humanities, Science & Engineering Research*. Kota Kinabalu, Sabah, Malaysia.